http://dx.doi.org/10.5012/bkcs.2014.35.7.1965

A New Adamantane-like Tetranuclear Manganese(III) Complex Based on Flexible Schiff-base Ligand: Synthesis, Crystal Structure and Magnetic Property

Ran Zhang, Zhong-Hai Ni, Li-Fang Zhang,* and Hui-Zhong Kou†,*

*School of Chemical Engineering and Technology, China University of Mining and Technology, Xuzhou 221116, Jiangsu Province, P.R. China. *E-mail: zhanglifang@cumt.edu.cn*
*†Department of Chemistry, Tsinghua University, Beijing 10084, P.R. China. *E-mail: kouhz@mail.tsinghua.edu.cn*
Received February 21, 2014, Accepted March 6, 2014

A new tetranuclear Mn(III) complex $[Mn^{III}_4(sae)_4(\mu_3\text{-}O)(\mu_{1,1}\text{-}N_3)(OH)(H_2O)_2]\cdot H_2O$ (**1**) (H_2sae = 2-salicylideneamino-1-ethanol) has been synthesized by the reaction of $MnCl_2\cdot 4H_2O$, H_2sae and sodium azide in the mixed solvent of methanol, acetonitrile and water. The X-ray diffraction analysis shows that the four Mn(III) ions in complex **1** have a unique adamantine arrangement, whereas the coordination environment of each Mn(III) ions is different. Magnetic studies indicate that complex **1** manifests antiferromagnetic behaviors. The magnetic susceptibilities of complex **1** have been fitted by two magnetic models based on the suitable analysis of its magnetic structural topology.

Key Words : Tetranuclear, Adamantine, Mn(III) complex, Schiff base, Magnetic property

Introduction

In the field of molecular magnetic materials, the famous manganese molecular clusters complexes $Mn_{12}O_{12}(CH_3CO_2)_{16}(H_2O)_4$ and its derivatives have attracted intense interest due to their relatively excellent single molecule magnets behaviors (SMMs).[1-4] Therefore, in very recent years, the synthesis and assembly of manganese multinuclear complexes with high-spin ground states and large magnetic anisotropy have been one hot topic for constructing new and amusing molecular magnets.[5-8]

Based on the understanding on the nature of magnetic coupling in Mn_{12}, new polynuclear manganese complexes containing oxygen bridges are more expected.[9] Along this idea, many new manganese clusters have been synthesized based on *O*-containing ligands and some of them interesting exhibit single molecule magnets behaviors.[10-12] The *O*-containing ligand used for the synthesis of polynuclear molecular clusters not only include classical carboxylic acid,[13] but also include Schiff base ligands,[14] phenolic ligands and their derivatives.[15] Among the numerous *O*-containing ligands, Schiff base ligands have attracted durative much attention because they manifest more diversity in assembly multinuclear complexes resulting from both nitrogen and oxygen atoms.[16,17]

Compared with the rigid Schiff base ligands, the flexible Schiff base ligands are more suitable for the assembly of polynuclear complexes with unique molecular structures and fascinating properties.[18] Up to date, several tens of clusters involving Ni^{II}, Cu^{II}, Fe^{II}, Fe^{III}, Mn^{II} and Mn^{III} ions based on flexible Schiff base ligands have been reported.[14,17,19-21] Recently, we selected a flexible Schiff base H_2sae as the main ligand, and small azide anion was introduced as the terminal or bridging ligand, a new adamantane-shaped tetranuclear Mn(III) complex with formula $[Mn^{III}_4(sae)_4(\mu_3\text{-}O)(\mu_{1,1}\text{-}N_3)(OH)(H_2O)_2]\cdot H_2O$ was synthesized. Herein, we report the synthesis, crystal structure and magnetic property of the title complex.

Experimental Section

Measurements. Elemental analyses (C, H and N) were carried out on an Elemental Vario E1 instrument. The infrared spectroscopy on Nicolet 7199B FTIR spectrophotometer in the 4000–400 cm^{-1} regions. Magnetic properties measurements on crystal samples were performed on a Quantum Design MPMS SQUID magnetometer. The experimental susceptibilities were corrected for the diamagnetism estimated based on Pascal's constants.

Synthesis of Complex 1. $MnCl_2\cdot 4H_2O$ (3 mmol) was added to a solution of H_2sae (3 mmol) in methanol (15 mL), the mixture was stirred at room temperature and then acetonitrile (10 mL) was added. To the above solution, an aqueous solution (5 mL) of NaN_3 (10 mmol) was added carefully. The resulting mixture was stirred for 15 min and filtered, the filtrate was left undisturbed at room temperature and brown cubic block crystals suitable for X-ray single crystal diffraction were obtained after several days. Yield: 60%. Elemental analysis calculated for: $C_{36}H_{41}Mn_4N_7O_{13}$, (999.52): C, 43.26; H, 4.13; N, 9.81%. Found: C, 43.23; H, 4.09; N, 9.83%. Selected IR frequencies (KBr disk, cm^{-1}): 3347, 2044 (νN_3), 2859 (νCH_2), 2938(νCH_2), 1625, 1600, 1541.

Crystal Structure Determination. Crystals data of complex **1** was selected on a Bruker APEX II CCDC diffractometer with graphite-monochromated Mo-Kα radiation (λ = 0.71073 Å) at 293 K using the ω-scan technique. The structure was solved by direct methods with the SHELXS-97 computer program, and refined by full-matrix least-squares methods (SHELXL-97) on F^2. Detailed information about the crystal data and structure determination for complex **1** is

Table 1. Crystal Data and Structure Refinement for **1**

Empirical formula(*M*)	$C_{36}H_{41}Mn_4N_7O_{13}$, (999.52)
Wavelength(Å)	0.71073
Crystal system	Monoclinic
space group	$P2_1/n$
a/b/c(Å)	17.814(4)/14.113(3)/19.762(4)
β(°)	114.949(17)
V(Å^3)	4504.7(16)
Z	4
D_{calc} (g cm^{-3})	1.474
μ(mm^{-1})	1.161
F(000)	2040
Crystal size (mm)	0.08 × 0.08 × 0.10
θ range for data collection (°)	3.10–25.00
Limiting indices	$-21 \le h \le 21$, $-16 \le k \le 16$, $-23 \le l \le 23$
Reflections collected/unique	32203/7815 [R(int) = 0.0729]
Reflections with I >2sigma(I)	6084
Data/restraints/parameters	7815/19/542
Goodness-of-fit on F^2	1.036
Final R indices [$I > 2\sigma(I)$]	R_1 = 0.0704, wR_2 = 0.1766
R indices (all data)	R_1 = 0.0642, wR_2 = 0.1899
Largest diff. peak and hole (e Å^{-3})	1.077 and −0.528

Table 2. Selected Bond Distances (Å) and Angles (°) for **1**

Mn(1)-O(1)	1.858(4)	Mn(3)-O(5)	1.881(3)
Mn(1)-O(2)	1.904(4)	Mn(3)-O(6)	1.935(3)
Mn(1)- O(4)	2.250(3)	Mn(3)-O(8)	2.236(3)
Mn(1)-O(6)	1.963(3)	Mn(3)-O(9)	1.889(3)
Mn(1)-O(1w)	2.359(6)	Mn(3)-N(3)	1.969(4)
Mn(1)-N(1)	1.986(4)	Mn(3)-N(5)	2.474(3)
Mn(2)-O(3)	1.876(3)	Mn(4)-O(2)	2.138(3)
Mn(2)-O(4)	1.876(3)	Mn(4)-O(7)	1.894(3)
Mn(2)-O(9)	1.876(3)	Mn(4)-O(8)	1.870(3)
Mn(2)-O(10)	2.267(4)	Mn(4)-O(9)	1.866(3)
Mn(2)-N(2)	1.954(4)	Mn(4)-N(4)	1.973(4)
Mn(2)-N(5)	2.474(4)	Mn(1)--Mn(2)	3.651(4)
Mn(1)--Mn(4)	3.590(4)	Mn(2)--Mn(3)	3.1368(11)
Mn(1)--Mn(3)	3.468(4)	Mn(2)---Mn(4)	3.513(4)
Mn(3)---Mn(4)	2.9707(11)		
Mn(2)-O(4)-Mn(1)	124.19(16)	Mn(4)-O(9)-Mn(2)	139.72(16)
Mn(3)-O(6)-Mn(1)	125.72(16)	Mn(4)-O(9)-Mn(3)	104.59(15)
Mn(4)-O(8)-Mn(3)	92.25(13)	Mn(2)-O(9)-Mn(3)	112.87(15)
Mn(2)-N(5)-Mn(3)	81.26(17)	Mn(1)-O(2)-Mn(4)	125.20(17)

summarized in Table 1. The selected bond distances and bond angles are given in Table 2. Crystallographic data for complex **1** has been deposited with CCDC-987816. This data can be obtained free of charge *via* www.ccdc.cam.ac.uk/conts/retrieving.html or from CCDC, 12 Union Road, Cambridge CB2 1EZ, UK. E-mail: deposit@ccdc.cam.ac.uk.

Results and Discussion

Crystal Structure of Complex 1. Single crystal X-ray diffraction analysis reveals that complex **1** crystallizes in monoclinic space group $P2_1/n$. The crystal structure of complex **1** is shown in Figure 1. Complex **1** has a adamantane-shaped structure consisting of four independent Mn(III) ions which were linked by four doubly deprotonated sae ligands, one azide anion and one oxygen atom. The coordination geometries of the four Mn(III) ions is shown in Figure 2. The crystal structure of complex **1** clearly shows that the coordination environments of four Mn(III) ions are different from each other, but it is in common that each of them has a trident sae ligand at equatorial plane. Mn(1) is coordinated by two oxygen atoms (O(1) and O(2)) and one nitrogen atom (N(1)) from the sae ligand and one oxygen atom (O(6)) from another sae ligand belongs to Mn(3) at the equatorial plane. Mn(1) and the four coordination atoms in the equatorial position are almost in the same plane with the maximum deviation of 0.051 Å (N(1)), the bond lengths of the Mn-O

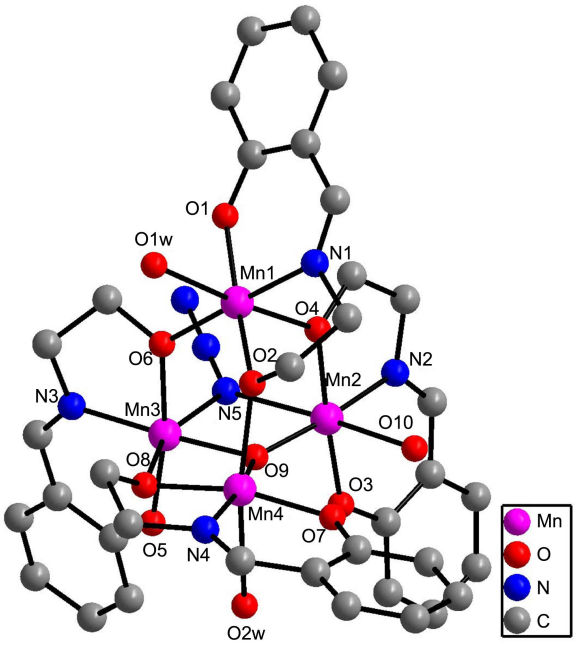

Figure 1. Molecular structure of complex **1**, free water molecules and hydrogen atoms are omitted for clarity.

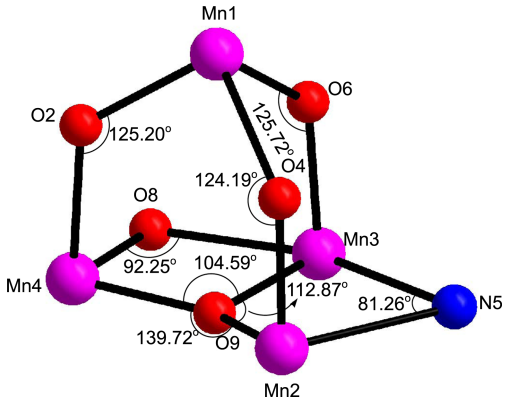

Figure 2. Adamantane-shaped structure formed by oxygen and nitrogen atoms linking four Mn(III) ions in complex **1** (Red for oxygen atom, pink for Mn atom and blue for nitrogen atom).

are range from 1.858(4) to 1.963(3) Å and Mn-N is 1.986(4) Å. At the axial position, Mn(1) is coordinated by one water molecule and one oxygen atom (O(4)) from the sae ligand which also coordinates to Mn(2) with the bond lengths of 2.359(6) Å for Mn(1)-O(1w) and 2.250(3) Å for Mn(1)-O(4), respectively. Mn(2) is bonded to two oxygen atoms (O(3) and O(4)) and one nitrogen atom (N(2)) from the sae ligand and one independent oxygen atom (O(9)) at the equatorial plane, which form a plane with a maximum deviation of 0.041 Å (O(9) and O(3)). Mn(2) is completed by one hydroxyl oxygen and one nitrogen atom (N(5)) from the bridging N_3^- ion at axial direction. Mn(3) is surrounded by two oxygen atoms (O(5) and O(6)) and one nitrogen atom (N(3)) from the sae ligand along with one independent oxygen atom (O(9)) at equatorial plane, which form a plane with a maximum deviation of 0.042 Å (O(9)) and a distance of 0.037 Å from Mn(3). Mn(3) is axially occupied by one oxygen atom (O(8)) from the sae ligand belongs to Mn(4) and one nitrogen atom (N(5)) from the bridging N_3^- ion. Mn(4) is chelated by two oxygen atoms (O(7) and O(8)) and one nitrogen atom (N(4)) from the sae ligand and one independent oxygen atom (O(9)) at the equatorial plane. Mn(4) is axially chelated by one oxygen atom (O(2)) from the sae ligand and weak-coordinated oxygen atom from water with the bond distance of Mn(4)-O(2w) = 2.751 Å. Finally, an elongated octahedral coordination environment is created for each Mn(III) ion. Thus, each of alcohol oxygen (O(2), O(4), O(6) and O(8) from the sae ligands is connected to the two Mn(III) ions. Furthermore, three Mn(III) ions are bridged by the independent O^{2-} (O(9)), the Mn(2) and Mn(3) ions are linked to N(5) from the bridging N_3^- ion. The co-connection of the three bridging modes formed the Mn_4O_4N adamantane structure of complex **1** (Figure 2).

Azide group in complex **1** is end-on type with the bond lengths of Mn(2)-N(5) = 2.474(4) Å, Mn(3)-N(5) = 2.474(3) Å, and the bridging angle Mn(2)-N(5)-Mn(3) is 81.26(17)°. The reason for the occurrence of such a low bridging angle is that the coordination of N(5) for Mn(2) and Mn(3) ions are axial. To the best of our knowledge, it is the lowest bridging angle for azide-bridged complexes. In the complex $\{[Mn^{III}_4(\mu_3\text{-}O)(sae)_4(\mu\text{-}N_3)(CH_3OH)_2]_2(\mu\text{-}N_3)\}(N_3)$, the bridging angle of azide with EO mode is 84.04(8)° which is considered as the lowest linking angle previously.[22] Azide ion is approximately linear with the bond angle of N(5)-N(6)-N(7) = 177.7(8)° in complex **1**. Other coordination bond lengths are in the normal range.[19,21,23,24] The shortest intramolecular distance between the two metal atoms is 2.9707(11) Å for Mn(3)---Mn(4). It is worth noting that the supramolecular structure of complex **1** is relatively simple due to the lack of relatively strong intermolecular interactions. Two clusters of complex **1** are linked together by π-π interactions between the two neighboring benzene rings, forming dimeric supramolecular structure (Figure S1).

Magnetic Properties. The magnetic susceptibilities of complex **1** have been measured in the temperature range of 1.8–300 K under the field of 1000 Oe. A pot of $\chi_m T$ and $1/\chi_m$–T *versus* T are shown in Figure 3, in which χ_m is molar

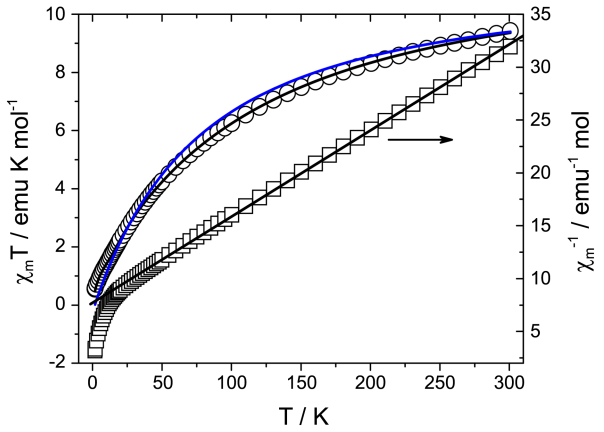

Figure 3. Curves of β_mT–T and $1/\beta_m$–T for complex **1** (The solid lines represent the best fitting based on the parameters discussed in the text).

susceptibility per Mn^{III}_4 unit. The $\chi_m T$ values of 9.42 emu K mol^{-1} at 300 K is lower than the spin-only values of 12.00 emu K mol^{-1} for four uncoupled Mn(III) ions based on g = 2.0, which is normal for antiferromagnetic systems with relatively strong antiferromagnetic coupling. On lowering the temperature, the $\chi_m T$ values relatively quickly decline to a minimum of 0.56 emu K mol^{-1} at 1.8 K. The changing tendency of this curve clearly suggests the existence of dominant antiferromagnetic coupling in complex **1**. The magnetic susceptibilities in the range of 25–300 K agree well with the Curie-Weiss law with a large negative Weiss constant θ = –94.59 K and Curie constant C = 12.27 emu K mol^{-1} which further confirms the presence of a stronger overall antiferromagnetic interactions in complex **1**. The magnetic field (H) dependence of magnetization (M) of complex **1** was measured at 1.8 K with fields up to 50 kOe. The data are presented in Figure 4 as plot of $M/N\beta$ (N represents Avogadro's constant, β is Bohr magneton) *versus* H. The experimental curve is far lower than the Brillouin curve with Lande factor g = 2.0, which also confirms the

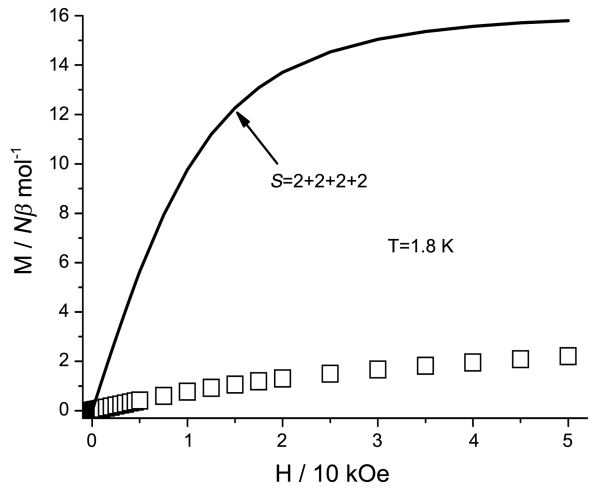

Figure 4. Field dependence of magnetization complex **1** (The line represents the Brillouin function based on g = 2.0 and four non-interacting Mn(III) ions).

overall antiferromagnetic interactions in complex **1**.

In complex **1**, the magnetic coupling between each pair of Mn(III) ions are extraordinary complicated due to the fact that the coordination environments of the four Mn(III) ions are different and the linkage of each pair of Mn(III) ions are not completely the same.

In order to qualitatively evaluate the magnitude of the magnetic interaction between the Mn(III) ions, the magnetic model of complex **1** was simplified by employing the same intramolecular magnetic coupling constant (J) for the comparatively complicated case. In addition, the intermolecular magnetic interaction (zJ') was taken into account.

On the basis of the regular tetrahedron arrangement of Mn^{III}_4 model (Scheme 1), the magnetic susceptibilities can be fitted accordingly by the following expressions given in Eqs. (1 and 2) derived from the spin Hamiltonian $\hat{H} = -2J(\hat{S}_1\hat{S}_2 + \hat{S}_1\hat{S}_4 + \hat{S}_2\hat{S}_3 + \hat{S}_3\hat{S}_4)$, where $A = 408\exp(48J/kT) + 840\exp(32J/kT) + 1092\exp(18J/kT) + 1100\exp(6J/kT) + 900\exp(-4J/kT) + 476\exp(-12J/kT) + 160\exp(-18J/kT) + 24\exp(-22J/kT)$, $B = 17\exp(48J/kT) + 45\exp(32J/kT) + 78\exp(18J/kT) + 110\exp(6J/kT) + 135\exp(-4J/kT) + 119\exp(-12J/kT) + 80\exp(-18J/kT) + 36\exp(-22J/kT) + 5\exp(-24J/kT)$.

$$\chi_t = \frac{Ng^2\beta^2}{kT}\frac{A}{B} \tag{1}$$

$$\chi_m = \frac{\chi_t}{1-\chi_t(2zJ'/Ng^2\beta^2)} \tag{2}$$

In which χ_t is molar susceptibility per Mn^{III}_4 unit only including intramolecular magnetic coupling, k is Boltzmann constant. The least-square fit of the experimental data in the whole temperature range to the above expressions gives the following parameters $J = -3.52(1)$ cm^{-1}, $g = 1.96(1)$, $zJ' = -0.12(2)$ cm^{-1}, $R = \Sigma[(\chi_mT)_{obsd.} - (\chi_mT)_{calcd.}]^2/\Sigma[(\chi_mT)^2_{obsd.}] = 8.72 \times 10^{-4}$. The small zJ' value suggests the intermolecular magnetic interaction is weak. The above fitting results for the magnetic susceptibilities of complex **1** seems acceptable based on the assumption that the four Mn(III) ions system accords with regular tetrahedron arrangement model (the blue line in Figure 3). However, the crystal structure parameters of complex **1** manifest that the coordination environments of four Mn(III) ions are largely different. Therefore, the above magnetic fitting model doesn't reflect the magnetic nature of complex **1**.

In order to obtain the main parameters which can better reflect the actual situation of magnetic coupling of complex **1**, we have carried out a very detailed analysis on the crystal structure parameters of complex **1** and referred to some relevant reports on the structural-magneto correlations of similar Mn(III) systems,[22] then offered an improved magnetic model for complex **1**.

According to the crystal structure parameters of complex **1**, the bond angles of Mn(1)-O(2)-Mn(4), Mn(2)-O(4)-Mn(1) and Mn(3)-O(8)-Mn(1) are close to each other, which indicates that the magnetic coupling constants should be very similar between Mn(1) and Mn(2), Mn(3), and Mn(4). Hence, it's reasonable to hypothesize that they have equal J_1 value. In addition, the bond angle of Mn(2)-O(9)-Mn(4) is 139.72(16)° which is obviously different with the angles mentioned above. Therefore, the magnetic coupling between Mn(2) and Mn(4) is another situation should be considered (J_2). Based on the reports of the literature,[22] the angles of Mn(4)-O(9)-Mn(3) and Mn(2)-O(9)-Mn(3) are approximately equal to 110° which is in the range of weak ferromagnetic coupling between neighboring Mn(III) ions. Moreover, the azide EO bridge transfers weak ferromagnetic coupling between Mn(2) and Mn(3)). In addition, there exists a Mn(3)-O(8)-Mn(4) magnetic coupling route between Mn(3) and Mn(4) with the angle of 92.25(13)° which also should be in the range of ferromagnetic coupling. However, the measurement results of magnetic susceptibility indicate that the complex **1** shows an overall antiferromagnetic coupling interaction, which can be due to that the antiferromagnetic coupling interactions between Mn(2) and Mn(4), and between Mn(1) and Mn(2), Mn(3), and Mn(4) are dominated. Therefore, it is reasonable to fit the magnetic property of complex **1** mainly considering the four strong antiferromagnetic coupling interactions (Scheme 2). The relatively weak

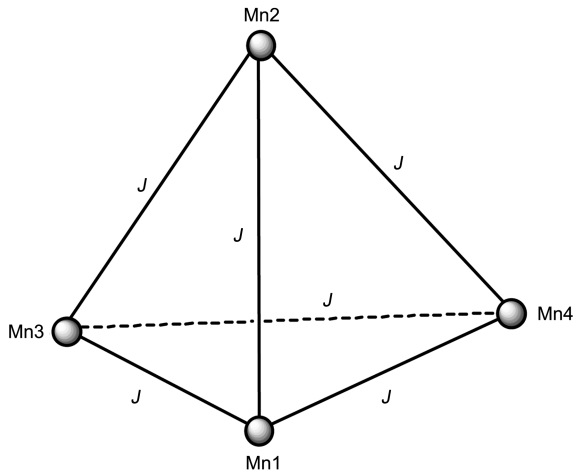

Scheme 1. Sketch map of magnetic coupling for regular tetrahedronal arrangement of Mn^{III}_4 system in complex **1**.

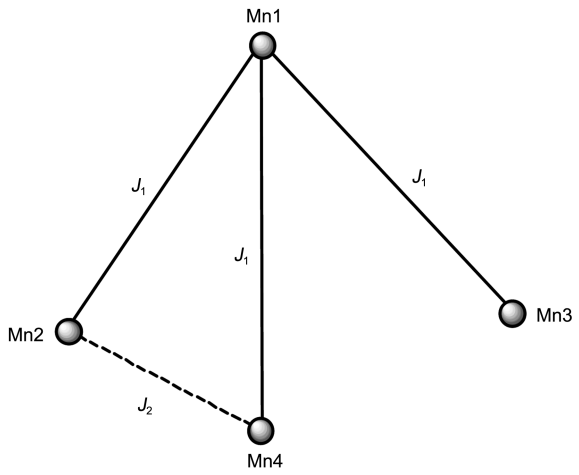

Scheme 2. Sketch map of critical magnetic coupling in complex **1**.

ferromagnetic coupling between Mn(2) and Mn(3) and between Mn(3) and Mn(4) together with the intercluster magnetic coupling can be classified to intermolecular interactions (zJ'). Moreover, it is easily to understand that the two ferromagnetic coupling interactions above mentioned are dominating in zJ'.

On the basis of the above Mn^{III}_4 model (Scheme 2), the magnetic susceptibilities of the title complex can be fitted accordingly by the below expression deduced from the spin Hamiltonian $\hat{H} = -2J_1\hat{S}_2(\hat{S}_1+\hat{S}_3+\hat{S}_4) - 2J_2\hat{S}_1\hat{S}_3 - J_1(\hat{S}^2-\hat{S}_B{}^2-\hat{S}_2{}^2) - J_2(\hat{S}_A{}^2-\hat{S}_1{}^2-\hat{S}_3{}^2)$, in which $S_A = S_1 + S_3$, $S_B = S_A + S_4$, $S = S_B + S_2$.

$$\chi_t = \frac{Ng^2\beta^2}{kT}\frac{A}{B} \tag{3}$$

$$\chi_m = \frac{\chi_t}{1-\chi_t(2zJ'/Ng^2\beta^2)} \tag{4}$$

Where, the detailed values of A and B see SI. The best-fit parameters obtained are $J_1 = -4.67(5)$ cm^{-1}, $J_2 = -5.14(8)$ cm^{-1}, $zJ' = 1.42(3)$ cm^{-1}, $g = 2.02(1)$, $R = 1.69 \times 10^{-5}$. The theoretical values conform to the experimental values (the black line in Figure 3) and the best-fit parameters are also very reasonable, which manifested that the model well reflects the actual coupling situation of complex **1**.

In the complex **1**, due to the $d_{x^2-y^2}$ orbit of the high-spin Mn(III)[d^4, $t_{2g}{}^3e_g$] ions have the highest energy, the four unpaired electrons occupied the four orbits of $d_{xy}(t_{2g})$, d_{xz} (t_{2g}), $d_{yz}(t_{2g})$ and $d_z{}^2(e_g)$, respectively. Based on the Kahn orbit model in complex **1**, the ferromagnetic (t_{2g} + eg) and antiferromagnetic ($t_{2g} + t_{2g}$) coupling coexist between the neighboring Mn(III) ions through oxygen atom bridge and the antiferromagnetic coupling contributions are dominated in the system. In addition, according to the spin polarization theory of the azido group, there may exist ferromagnetic coupling interaction between Mn(III) ions through EO azide bridge in complex **1**, but in general the ferromagnetic coupling interaction is too much weak to atonement the net contribution of antiferromagnetic coupling bridged by oxygen atom between Mn(III) ions. According to the above described results, we can see that the complex **1** exhibits overall antiferromagnetic coupling.

Conclusion

In summary, we have synthesized a new tetranuclear manganese(III) adamantane-like complex $[Mn^{III}_4(sae)_4(\mu_3\text{-}O)(\mu_{1,1}\text{-}N_3)(OH)(H_2O)_2]\cdot H_2O$ based on Schiff base ligand. The coordination environments of four Mn(III) ions are different from each other. The magnetic measurement indicated the presence of overall antiferromagnetic interaction in the title complex. The magnetic susceptibilities of the title complex have been fitted by two magnetic models based on the suitable analysis of its magnetic structural topology.

Acknowledgments. This work was supported by a Project Funded by the Priority Academic Program Development of Jiangsu Higher Education Institutions, the Natural Science Foundation of Jiangsu Province and the Fundamental Research Funds for the Central Universities (2013QNA17).

Supplementary Materials. The dimeric supramolecular structure Figure, the powder XRD Figure and the fitting expression for magnetic susceptibilities and the CIF file of the title complex can be found.

References

1. Novoa, J. J.; Deumal, M.; Jornet-somoza, *J. Chem. Soc. Rev.* **2011**, *40*, 3182.
2. Zhang, P.; Guo, Y.-N.; Tang, J. *Coord. Chem. Rev.* **2013**, *257*, 1728.
3. Sessoli, R.; Gatteschi, D.; Caneschi, A.; Novak, M. A. *Nature* **1993**, *365*, 141.
4. Thomas, L.; Lionti, F.; Ballou, R.; Gatteschi, D.; Sessoli, R.; Barbara, B. *Nature* **1996**, *383*, 145.
5. Cavallini, M.; Gomez-Segura, J.; Ruiz-Molina, D.; Massi, M.; Albonetti, C.; Concepci, C.; Rovira, C.; Veciana, J.; Biscarini, F. *Angew. Chem. Int. Ed.* **2005**, *44*, 888.
6. Yoo, J.; Wernsdorfer, W.; Yang, E. C.; Nakano, M.; Rheingold, A. L.; Hendrickson, D. N. *Inorg. Chem.* **2005**, *44*, 3377.
7. Chakov, N. E.; Wernsdorfer, W.; Abboud, K. A.; Christou, G. *Inorg. Chem*. **2004**, *43*, 5919.
8. Ge, C. H.; Ni, Z. H.; Liu, C. M.; Cui, A. L.; Zhang, D. Q.; Kou, H. Z. *Inorg. Chem. Commun.* **2008**, *11*, 675.
9. Shah, S. J.; Ramsey, C. M.; Heroux, K. J.; DiPasquale, A. G.; Dalal, N. S.; Rheingold, A. L.; Barco, E.; Hendrickson, D. N. *Inorg. Chem.* **2008**, *47*, 9569.
10. Lecren, L.; Roubeau, O.; Coulon, C.; Li, Y. G.; Le Goff, X. F.; Wernsdorfer, W.; Miyasaka, H.; Clérac, R. *J. Am. Chem. Soc*. **2005**, *127*, 17353.
11. Yang, C.; Wang, Q. L.; Su, C. Y.; Hu, L. N.; Li, L. C.; Liao, D. Z. *Inorg. Chem. Commun*. **2014**, *40*, 26.
12. Yang, P. P.; Song, X. Y.; Liu, R. N.; Li, L. C.; Liao, D. Z. *Dalton. Trans*. **2010**, *39*, 6285.
13. Sivanesan, D.; Son, K.; Lee, H. J.; Park, K. T.; Jang, Z.; Suh, B. J.; Yoon, S. *Polyhedron* **2013**, *50*, 339.
14. Zhang, L. F.; Ni, Z. H.; Zong, Z. M.; Wei, X. Y.; Ge, C. H.; Kou, H. Z. *Acta Cryst.* **2005**, *61*, 542.
15. Yang, E. C.; Harden, N.; Wernsdorfer, W.; Zakharov, L.; Brechin, E. K.; Rheingold, A. L.; Christou, G.; Hendrickson, D. N. *Polyhedron* **2003**, *22*, 1857.
16. Oshio, H.; Hoshino, N.; Ito, T. *J. Am. Chem. Soc.* **2000**, *122*, 12602.
17. Oshio, H.; Hoshino, N.; Ito, T.; Nakano, M.; Renz, F.; Gütlich, P. *Angew. Chem. Int. Ed.* **2003**, *42*, 223.
18. Yang, X. P.; Chan, C.; Lam, D.; Schipper, D.; Stanley, J. M.; Chen, X. Y.; Jones, R. A.; Holliday, B. J.; Wong, W. K.; Chen, S. C.; Chen, Q. *Dalton Trans.* **2012**, *41*, 11449.
19. Boskovic, C.; Bircher, R.; Tregenna-Piggott, P. L. W.; Güdel, H. U.; Paulsen, C.; Wernsdorfer, W.; Barra, A. L.; Khatsko, E.; Neels, A.; Stoeckli-Evans, H. *J. Am. Chem. Soc.* **2003**, *125*, 14046.
20. Lu, Z. L.; Fan, T.; Guo, W. W.; Lu, J.; Fan, C. H. *Inorganica Chimica Acta* **2013**, *400*, 191.
21. Oshio, H.; Nihei, M.; Yoshida, A.; Nojiri, H.; Nakano, M.; Yamaguchi, A.; Karaki, Y.; Ishimoto, H. *Chem. Eur. J.* **2005**, *11*, 843.
22. Hoshino, N.; Ito, T.; Nihei, M.; Oshio, H. *Inorg. Chem. Commun.* **2003**, *6*, 377.
23. Miyasaka, H.; Nezu, T.; Sugimoto, K.; Sugiura, K. I.; Yamashita, M.; Clérac, R. *Chem. Eur. J.* **2005**, *11*, 1592.
24. Nihei, M.; Hoshino, N.; Ito, T.; Oshio, H. *Polyhedron* **2003**, *22*, 2359.